MODEL-BASED ANALYSIS OF THE DYNAMIC BEHAVIOUR
OF A 250 KN SHOCK FORCE CALIBRATION DEVICE

Michael Kobusch, Leonard Klaus, and Thomas Bruns

Physikalisch-Technische Bundesanstalt (PTB), Bundesallee 100, 38116 Braunschweig, Germany,
michael.kobusch@ptb.de

Abstract: An analysis of the dynamic behaviour of the 250 kN primary shock force calibration device at PTB is presented. Two airborne mass bodies with the force transducer under test are brought to collision, and the generated inertial forces are determined by means of laser vibrometers. Measurements with a heavy transducer revealed modal oscillations which were identified by acceleration sensors. The dynamic system behaviour was analysed with a finite element model. It showed that the elastic coupling between the transducer and the reference mass body causes low-frequency oscillations that have to be taken into account for calibration purposes.

Keywords: shock force calibration, impact bodies, inertial forces, dynamic modelling.

1. INTRODUCTION

In recent years, the measurement of dynamic forces has gained considerably in importance in many industrial areas. Rising numbers of dynamic applications and increasingly higher demands on measurement accuracy set new metrological challenges. Due to the lack of documentary standards or commonly accepted guidelines for force measurements under dynamic conditions, the traceability of force is still purely based on static calibrations, which means that dynamic loads may not be measured correctly. To research and provide metrological traceability for dynamic force measurements, which is highly important for future metrology, PTB has developed several primary calibration facilities operating with sinusoidal or shock excitation.

For shock force calibrations of even large and heavy transducers up to 250 kN force amplitude, a new primary calibration device has been presented in 2010. Its mechanical design and specifications are described in detail in [1]. Figure 1 shows a photograph of this shock force calibration device, and Fig. 2 depicts a corresponding sketch.

Shock forces are generated by a collinear collision of two cylindrical reference mass bodies of 100 kg that are guided by air bearings to minimize friction. A computer-controlled hydraulic drive accelerates the impacting mass body M1 to its impact velocity (range 0.02 m/s to 1.5 m/s) before it hits the force transducer under test mounted on the second body M2, which is initially at rest. After the collision

and momentum transfer, the remaining kinetic energy of both impact partners is absorbed by dampers.

The generated inertial forces during the time of collision are determined by means of two laser-Doppler interferometers (vibrometers) which simultaneously probe the bodies' front faces on their common axis of motion. With Newton's second law defining the inertial force of an accelerated mass body, traceability of the shock force measurement is realised by the determination of mass (from weighing) and acceleration (by means of the laser vibrometers). The duration and spectral content of the generated force pulse can be varied by applying impact plates of different stiffness.

Fig. 1. 250 kN shock force calibration device.

First shock measurements [1] with a heavy 225 kN strain gauge force transducer weighing about a quarter of the coupled reference mass body revealed strong modal oscillations that have to be fully explained and properly considered for the development of suitable calibration methods. In general, the shorter the shock pulses, the more pronounced the excited modal oscillations. This means that short pulses are especially well suited to analyse and understand the dynamic behaviour of the calibration device.

In the following, the origins of these resonances are experimentally identified and confirmed by means of a finite element analysis of the mechanical impact configuration of the shock force calibration device. In continuation of the first tests, the investigations described in this paper were performed with the same force transducer.

2. MECHANICAL STRUCTURE

The investigated impact configuration consists of the two cylindrical reference mass bodies M1 and M2, the force transducer under test and several adaptation parts. Figure 2 gives a sketch of the axisymmetric geometry of this mechanical structure. The impacting mass body M1 is shown at the right, the reacting body M2 with the mounted transducer at the left. Both bearing seats have a diameter of 240 mm.

The trailing end face of the impacting mass body M1 features a flange ring as part of a braking mechanism with circularly arranged dampers fixed at the air bearing housing. An interchangeable impact plate made of hardened steel and a beam target plate with a retro-reflector are mounted by central threads.

The force transducer under test is a shear beam type strain gauge transducer. It consists of a low profile load cell and a base adapter (both coloured in blue, cf. Fig. 7) which are connected by 16 bolt screws. Central threads at both ends of the transducer intercept a hardened load button with a spherical cap and the adapter to mount this mechanical configuration at the reference mass body M2. The leading end face of M2 carries a second beam target plate for the second interferometer.
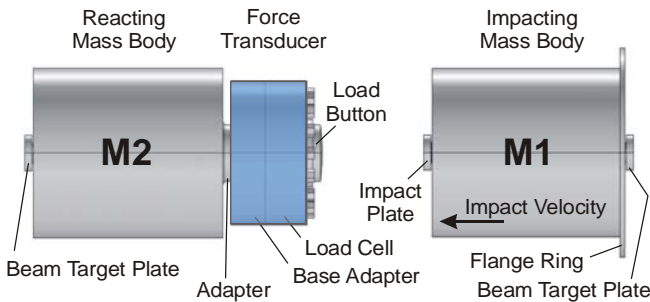

Fig. 2. Mechanical structure of the calibration device with mounted 225 kN strain gauge force transducer.

3. EXPERIMENTAL ANALYSIS OF MODAL OSCILLATIONS

A typical example measurement that demonstrates impact-excited modal oscillations is given in Fig. 3. The two diagrams visualize a shock force pulse of 37 kN peak amplitude in the time and frequency domain. As no pulse shaper was inserted between the colliding bodies, the hard metallic impact resulted in a short pulse of 1.2 ms pulse duration. Three measured force signals are displayed: the force transducer (FT) using its static sensitivity and the two inertial forces of both mass bodies (M1, M2) derived from interferometric measurements. Several modal oscillations can be clearly distinguished in the time domain, where a 10 kHz low-pass filter has been applied. The spectral analysis provides further information about the involved frequency components.

The lowest most prominent frequency components of the force transducer signal are at about 1.4 kHz and 6 kHz. The inertial force of the connected mass body M2 also contains these frequency components, but there are additional strong components at higher frequencies. For the inertial force of the impacting mass body M1, the first strong component appears at 9 kHz.
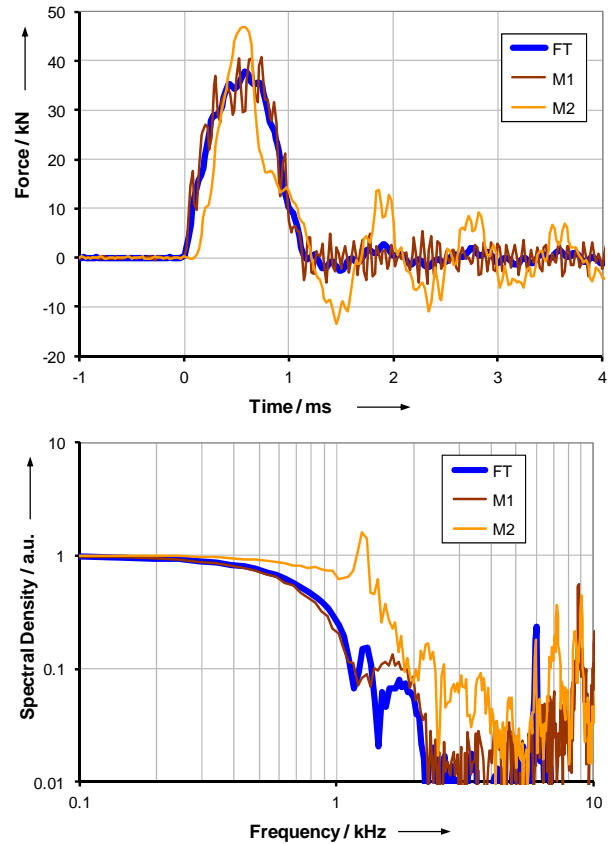

Fig. 3. Shock force measurement with excited modal oscillations: time domain (above), frequency domain (below), force transducer FT, inertial force of mass body M1, M2.

The detected modal oscillations most probably result from resonances of large structural mass components in association with elasticities of comparably weak stiffness. Possible causes might be the oscillation of the force transducer set-up against its sustaining mass body M2, the oscillation of the transducer's head mass or modal oscillations of the protruding flange ring, respectively. The mode at 6 kHz is probably caused by the vibration of the transducer's top mass, as the datasheet of the 225 kN force transducer specifies a fundamental resonance of 5.8 kHz.

To pinpoint the origins of the various modal oscillations, the measuring set-up was applied with additional acceleration sensors. Small sensors of a mass of 0.7 g and dimensions of Ø 6 mm x 8 mm were fixed at interesting measurement points by means of bonding wax. The comparison of the different acceleration amplitudes and phase relations gives some indications to the modal shape of the observed oscillations, which are subsequently confirmed by means of a finite element modelling.

The experimental results from different shock force measurements as well as hammer excitations are described in the following.

3.1 Modal analysis of the impacting mass body M1

Figure 4 shows a photo of the experimental set-up for the modal analysis of the impacting mass body M1. In this context it was suspected that the protruding flange ring might cause modal oscillations affecting the effective inertia force transmitted during impact.

Fig. 4. Mass body M1 applied with additional acceleration sensors.

Various tests were performed using three additional acceleration sensors applied at the structure at different points of interest. The test configurations are listed in the following.

1. Impact shock test with three acceleration sensors at the flange ring (sensor S1), at the rear (S2) and front face (S3) of the mass body near the centre.
2. Impact shock test with three acceleration sensors at the flange ring equally spaced around the circumference or side by side.
3. Configuration as before, but hammer excitation of the flange ring.

Impact shock tests with the colliding mass bodies prove a strong resonance of the flange ring at 4.8 kHz and a weaker resonance at 8.8 kHz. Figure 5 presents an FFT analysis of the ringing of the three acceleration signals. The spectral resolution is 0.05 kHz, the data sample started 10 ms after the onset of the shock pulse. The resonance line of the flange is not found in the spectrum of the other sensors (S2, S3) mounted at rear and front face.

At 8.8 kHz, the rear and front faces of the mass body oscillate in opposite directions (phase difference of 180°). For this reason, this resonance likely corresponds to a longitudinal vibration mode of the cylindrical mass body.

In case of a hammer excitation, the spectral content of the ringing of the flange ring acceleration signals is totally different as a comb of 8 resonances appears in the frequency range up to 10 kilohertz (see Fig. 6). However, it shows that these modes are not excited to any considerable extent under impact conditions because of the structural symmetry.

The experiments prove that impact-excited modal oscillations of the flange ring likely will not compromise the traceability of the interferometric determination of the inertia force of the impacting mass body.
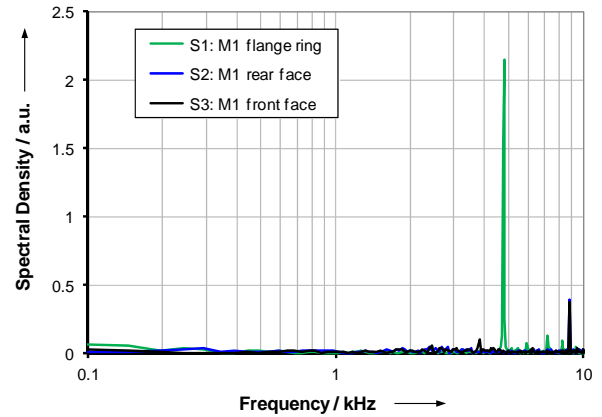

Fig. 5. Amplitude spectrum of the signal ringing of the accelerations at M1 for impact shock excitation.
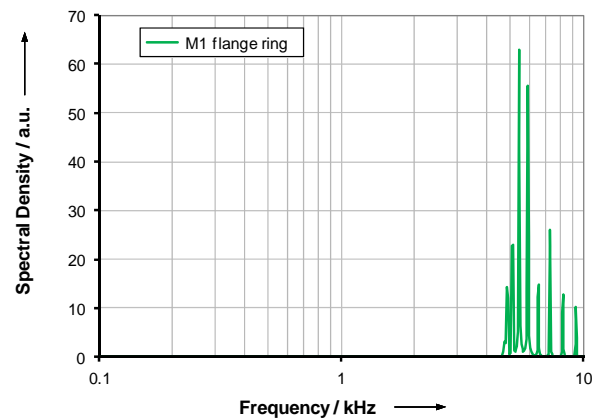

Fig. 6. Amplitude spectrum of the signal ringing of the acceleration at the M1 flange ring obtained with hammer excitation.

3.2 Modal analysis of the reacting impact partner

Figure 7 shows the set-up for the experimental modal analysis of the reacting mass body M2 with the mounted force transducer under test. Four additional acceleration sensors were again applied at different points of interest. The following test arrangements and tasks were chosen:

1. Impact shock test with three acceleration sensors mounted at the force transducer: one sensor (S1) at the transducer's head mass next to the load button, the second sensor (S2) at the top of the transducer housing (load cell), the third (S3) at the transducer's base adapter. The fourth sensor (S4) was attached to the reacting mass body M2.
2. Additional tests with pulse shapers to achieve longer pulse durations.
3. Impact shock test with acceleration sensors attached to the head mass (S1), the transducer housing (S2), the rear (S3) and front face (S4) of the mass body M2.
4. Variation of the mounting torque of the two adapter threads that connect transducer and mass body (cf. Fig. 2).

The first arrangement demonstrates that the two sensors S2 and S3 mounted at the opposing faces of the force transducer housing show almost identical signals in the time and frequency domain. Therefore, the load cell and the base adapter of the transducer behave as a rigid body in the considered frequency range up to 10 kHz.
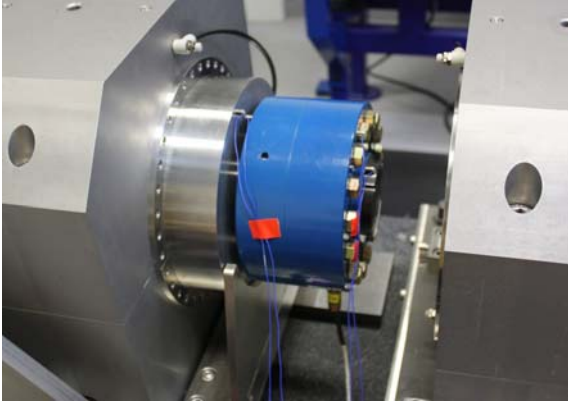
Fig. 7. Mass body M2 with 225 kN force transducer under test applied with additional acceleration sensors for modal analysis.

All tests clearly demonstrate two dominant resonances at about 1.4 kHz and 6.0 kHz. Both modes can be identified in the acceleration signals except for very smooth and long force pulses achieved with appropriate pulse shapers.

With the use of the third arrangement, Figure 8 shows typical acceleration signals of an impact shock excitation in the time domain. Figure 9 additionally visualizes the signal ringing in the frequency domain.
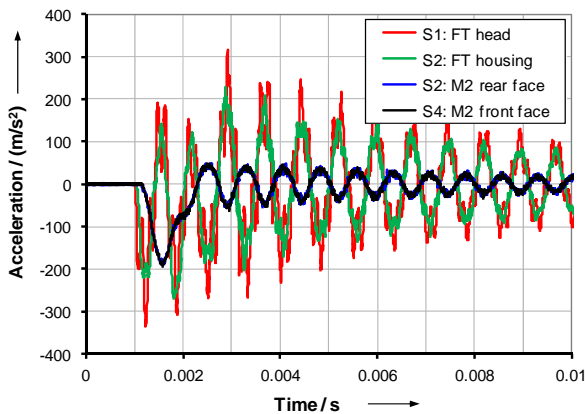

Fig. 8. Accelerations of four measurement points on the reacting impact partner.
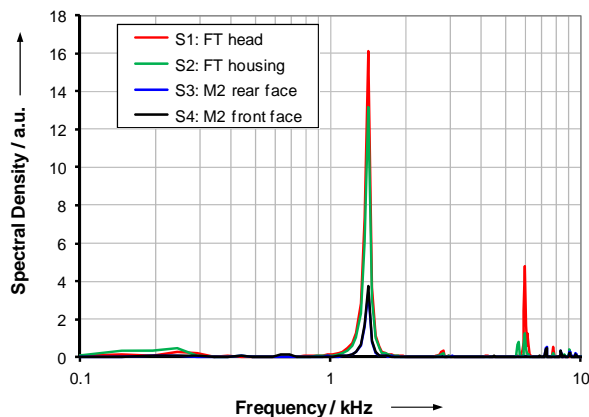

Fig. 9. Amplitude spectrum of the signal ringing of the acceleration signals of the previous plot.

The time plot clearly demonstrates that the sensors attached to the force transducer (S1, S2) experience an out-of-phase vibration at 1.4 kHz with respect to the sensors fixed at the mass body (S3, S4). This measurement proves the suspected resonance of the coupled large masses of force transducer and mass body.

The resonance at 6.0 kHz is predominately strong at the head mass of the force transducer. Here, the head and the housing of the force transducer oscillate in opposite directions, i.e. this mode is identified as the resonance of the transducer's head mass. The measured value agrees well with the specified resonance frequency.

There are few other weak resonances below 10 kHz which still need to be identified if necessary. This probably would need more experimental data as well as support by a finite element modelling which is described in the following section.

After having identified the origins of the two strongest modal oscillations, a possible influence on screw mounting torque was experimentally investigated using the fourth test arrangement. It showed that the resonance frequency at 1.4 kHz significantly increases with higher mounting torques. This behaviour was observed for both screw connections, and a value of 1.58 kHz was measured for the largest mounting torques applied. The investigations on the influence of the mounting torque on the dynamic behaviour of the shock force calibration will continue. To describe the dynamic behaviour by means of an appropriate model, qualified model descriptions and parameter values for the stiffness and the damping properties of the compound mechanical structure have to be found and evaluated.

4. MODELLING

The dynamic behaviour of the impact configuration shown in Fig. 2 is analysed and modelled by means of two different model approaches. A finite element modelling which describes the geometric structure with its three-dimensional distribution of mass, elasticity and damping is performed in order to identify the measured modal oscillations and to characterize the less known coupling properties. A simplified spring-mass-damper model with discretized bodies might then be applied in order to simulate the response to impact shock forces.

4.1 Finite element modelling

A finite element analysis of the modal oscillations was performed with the software COMSOL Multiphysics. The geometry of the modelled mechanical structure including the transducer under test (see Fig. 2) is known from engineering drawings. Greater uncertainties in the model description are attributed to the less known material parameters, but in particular, to the poorly known stiffness and damping properties of the screw connections of the various mechanical parts. The modal analysis presented in this paper assumes firm contact between connected partners, without considering any contact surfaces and friction. Mechanical assemblies are thus described by a single solid body of appropriate geometry.

The calculated eigenfrequencies and mode shapes of the impact configurations consisting of the two impact partners are presented in the following figures. The numerical results are discussed in consideration of the measured results previously described. As the axisymmetric structural geometry and impact geometry would not effectively excite modes which are not axisymmetric, e.g. bending modes of the mass body or the transducer, these modes are not of great importance and need not to be considered in detail.

Figure 10 presents the deformed geometry of three axisymmetric modal oscillations of the impacting mass body M1 below 10 kHz. The geometry deformation plots apply a default scale factor and a surface colour palette which automatically scales from minimum (blue) to maximum (red) surface displacement in axial direction.
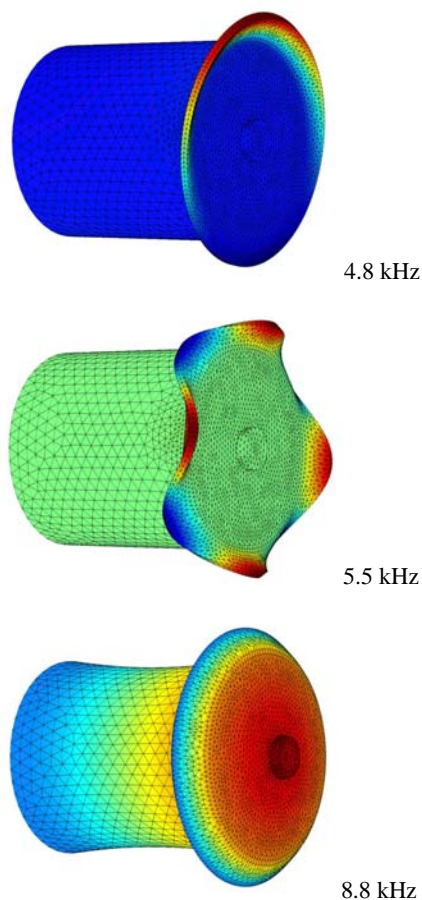

4.8 kHz

5.5 kHz

8.8 kHz

Fig. 10. Axisymmetric modal oscillations of the mass body M1 at 4.8 kHz, 5.5 kHz and 8.8 kHz.

The first mode of the mass body M1 appears at 4.8 kHz. At this frequency, the flange ring exhibits an axisymmetric warping. This numerical result nicely agrees with the measured resonance shown in Fig. 5.

The second mode image visualizes one of many bending modes of the flange ring with following eigenfrequencies: 4.9 kHz, 5.2 kHz, 5.5 kHz, 6.0 kHz, 6.6 kHz, 7.4 kHz, 8.4 kHz, and 9.5 kHz. These values perfectly agree with the mode comb experimentally observed for hammer excitations (cf. Fig. 6).

The third mode at 8.8 kHz represents the first longitudinal oscillation, which was also experimentally confirmed (cf. Fig. 5).

The FE results for the reacting mass body M2 with the mounted force transducer are presented in Figure 11. The two axisymmetric modes at 1.9 kHz and 6.1 kHz correspond to the measured resonances of 1.4 kHz (1.6 kHz for higher mounting torque) and 6.0 kHz described in the previous section. Furthermore, the first bending mode of the coupled heavy masses was calculated to be in the order of 300 Hz.

Whereas the calculated value for the modal oscillation of the transducer's head mass is in excellent agreement with the measurements, the FE analysis calculates substantially higher frequency values for the axial resonance of the coupled large masses. Obviously, the FE model has to be modified to accurately describe the screw connections, or the experiments could achieve better agreement for much higher mounting torques, respectively. Future work will help to clarify this discrepancy.
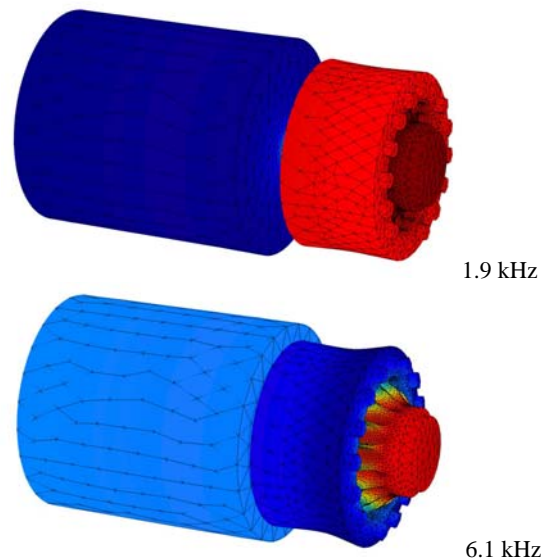

1.9 kHz

6.1 kHz

Fig. 11. Axisymmetric modal oscillations of the mass body M2 and the coupled transducer at 1.9 kHz and 6.1 kHz.

4.2 Discretized multi-body model

To simulate the dynamic behaviour of the impacting mass bodies and to predict the dynamic signals which will be experimentally measured, it is intended to model the mechanical impact configuration by means of a discretized multi-body model of one dimension, consisting of a linear arrangement of rigid masses coupled by elastic springs and dampers.

In this model, the force transducer to be calibrated forms an integral part of the calibration device and is described by model parameters (head mass m_H, base mass m_B, stiffness k, damping d) that define the transducer's dynamic response on dynamic loads. Experiences with acceleration sensors, which have a closely related mechanical design, have shown that such a model-based calibration approach consistently describes the dynamic measurement performance and is able to link measurement results from different calibration devices, independent of the applied dynamic excitation
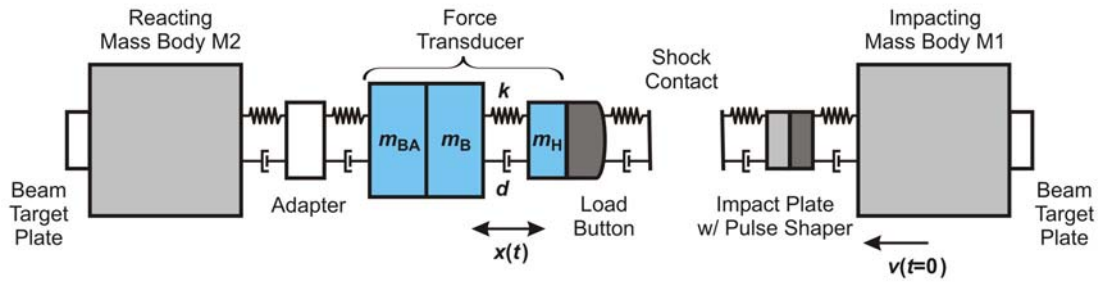
Fig. 12. Multi-body model of the shock force calibration device,
reacting mass body M2 with the force transducer (left), impacting mass body M1 (right).

forms, e.g. sine or shock [2]. First tests with force transducers showed that this model approach may be also applied to force transducers [3].

An appropriate multi-body model of the shock force calibration device is exemplarily depicted in Fig. 12. The model consists of a series arrangement of numerous mass-spring-damper systems. This model should be able to describe the dynamic behaviour of the numerous elastically coupled mechanical parts in uniaxial motion. The coupling between the two impacting partners will be either described by (measured) contact forces or by a non-linear contact model (Hertzian contact).

5. CONCLUSIONS AND OUTLOOK

This paper presents the model-based analysis of the dynamic behaviour of the 250 kN primary shock force calibration device at PTB. The investigations were performed with a force transducer of 225 kN capacity. The modal oscillations of the impact configuration were experimentally determined by tests with short shock pulses. A modelling with finite elements gave good agreement and a profound understanding of the modal oscillations that may occur. It was found that the finite element modelling needs some refinement in order to obtain better agreement in those cases where screw connections play an important role for the dynamic behaviour. In addition, a discretized multi-body model was introduced which is capable to simulate the dynamic behaviour of the shock force calibration device for uniaxial motion.

Further research on shock modelling with finite element methods is desired in order to get a sound understanding of the impact dynamics. The establishment of an improved measurement uncertainty budget for shock force calibrations would probably benefit from these investigations.

Research on the dynamic measurement of mechanical quantities including dynamic force is a current research topic of the EMRP Joint Research Project IND09 [4]. This research will finally provide the metrological foundation for future recommendations, guidelines and documentary standards on dynamic shock force measurements.

ACKNOWLEDGEMENTS

REFERENCES

[1] M. Kobusch, T. Bruns, L. Klaus, M. Müller, "The 250 kN primary shock force calibration device at PTB", Measurement, Special Issue: IMEKO 2010 Pattaya, Elsevier, to be published.

[2] T. Bruns, A. Link, C. Elster, "Current developments in the field of shock calibration", XVIII IMEKO World Congress, Rio de Janeiro, Brazil, 2006.

[3] M. Kobusch, A. Link, A. Buss, T. Bruns: "Comparison of shock and sine force calibration methods", Proc. of IMEKO TC3 & TC16 & TC22 International Conference, Merida, Mexico, 2007.

[4] C. Bartoli, F. Beug, T. Bruns, C. Elster, T. Esward, L. Klaus, A. Knott, M. Kobusch, S. Saxholm, and C. Schlegel, "Traceable dynamic measurement of mechanical quantities: objectives and first results of this European project", XX IMEKO World Congress, Busan, Republic of Korea, 2012, to be published.